

## Research Article

Ralf Biertümpfel\* and Steffen Reichel

# NIR cutoff filter for true color imaging sensors

**Abstract:** The function of a near-infrared (NIR) cutoff filter for imaging sensors is being described. The main purpose of the NIR cut filter is to obtain correct color recognition; therefore, the NIR filter is made of an absorbing filter glass and an interference coating. The absorbing filter glass is needed to minimize multiple reflections inside the lens system, which are the cause for ghost images. An additional interference coating enhances the function of the filter. Coating and filter glass are strongly dependent on each other. This requires high reproducibility and low tolerances of the filter glass and interference coating. In addition, features like inner quality – especially striae – and stability of the refractive index are important. A NIR cut filter may be designed as a flat plate or as a lens. Our analysis provides an estimation about striae level and variation of transmittance and their effect on image quality and color recognition. Furthermore, the use of an absorption filter glass as a lens (shrinking down the overall size) is discussed in terms of the influence on transmission and striae.

**Keywords:** absorption filter; color recognition; imaging sensor; lens; NIR cut filter; refractive index; striae; true color.

**OCIS code:** 220.0220.

\*Corresponding author: Ralf Biertümpfel, SCHOTT AG, Advanced Optics Hattenbergstr. 10, 55122 Mainz, Germany, e-mail: ralf.biertuempfel@schott.com

Steffen Reichel: SCHOTT AG, Advanced Optics Hattenbergstr. 10, 55122 Mainz, Germany

## 1 Introduction

The color recognition of the human eye uses three different wavebands of the visible spectrum. These sensitivity functions of the human eye are called color-matching functions, and they were standardized in 1931 by CIE [1]. Figure 1 depicts the color-matching functions of a standard colorimetric observer with a visual field of 2°.

Modern imaging sensors use a matrix of printed organic filters for color recognition. Each printed filter is positioned above a corresponding pixel of the CCD or CMOS sensor. However, the spectral response of such a filter-pixel combination is different from the color-matching functions of the human eye. A typical spectral response of such a native color pixel is shown in Figure 2 (data taken from [2]). It can easily be seen that the spectra are very different: The digital camera can detect a much greater range of wavelengths than the human eye. Additionally, the organic color pixels have an ambiguity for wavelengths >670 nm. This means, in case light with a wavelength of, e.g., 850 nm hits the sensor, the camera cannot calculate the correct color for the human color recognition, as the human eye is only sensitive to about 780 nm.

Therefore, an additional filter has to be used, which blocks all light with wavelengths longer than 670 nm (see Figure 3). Such a filter transmits only wavelengths to the color analysis of the camera, which are useful for the human color perception.

## 2 Ghost images are reduced by absorption filters

Such filters are many times manufactured as pure interference filters due to cost reasons. However, an interference coating has two main disadvantages, which cause ghost images and haze in a lens system:

1. Any interference coating is strongly dependent on the angle of incidence, and it is often optimized for small angles of incidence (<25°).
2. The blocking function of an interference filter works by reflection. That means, all unwanted light is reflected back into the lens system (see Figure 4). This reflected light will be reflected again at the other surfaces of the lens system (because the AR coatings of the lenses are usually optimized for the visible range of wavelengths up to 670 nm).

Thus, there are multiple reflections of the light, which has wavelengths longer than 670 nm. This multiple reflected

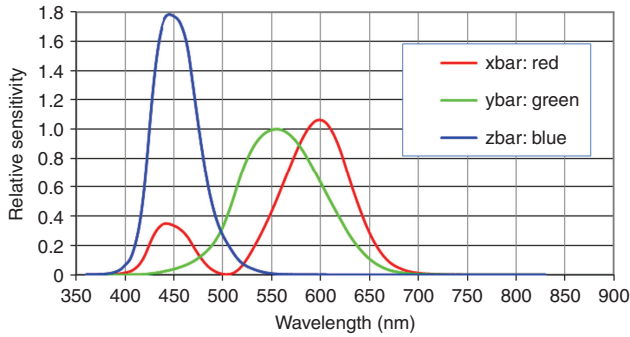


**Figure 1** Spectra of the color-matching functions of a standard colorimetric observer at 2° visual field according to CIE 1931 [1].

light hits the filter now at a different angle of incidence (which is >25°) and can easily pass the filter. Figure 5 displays this effect: the graph shows the spectral transmittance of a pure interference filter with an optical glass (N-BK7) as a substrate. The design was optimized for angles of incidence between 0° and 20°. For angles of incidence >20°, there is a significant increase in transmittance for NIR radiation from 900 nm on.

Figure 6 shows ghost images of the hot region of a flame. The ghosts are upside down and of false color because of the mistaken calculation of the camera’s color algorithm caused by NIR light.

### 3 High-performance NIR cut filter

For better image quality, an optimized optics design requires a combination of both an absorbing filter and an additional interference filter for NIR blocking. In addition, an AR coating increases the overall power transmission. The absorbing filter glass dissipates the unwanted light into heat without the reflection of light back into the lens

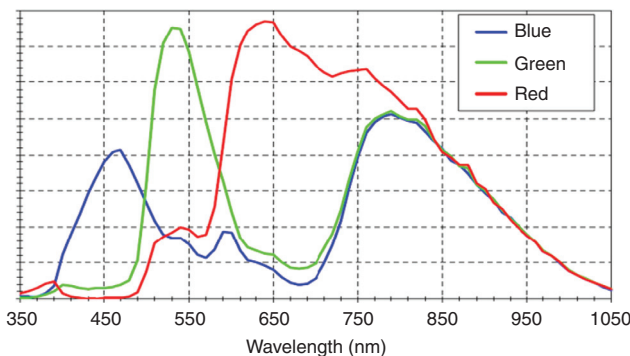


**Figure 2** Spectra of the response of native color pixels of a typical digital sensor, which has a sensitivity between 300 nm and 1100 nm. Source [2].

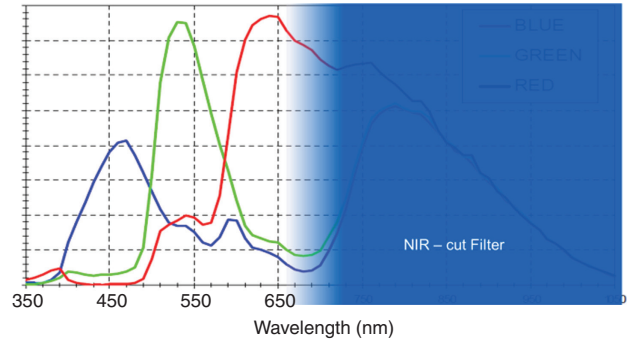


**Figure 3** Illustration of the blocking function of a NIR cutoff filter, which has a region of high transmittance in the range of wavelengths that can be analyzed for human color recognition.

system. However, typical absorbing filters are limited in their properties: there is no sharp transition between the visible region of high transmittance and the region of high absorption (see Figure 7). Additionally, the ratio between high transmittance and high absorption is not big enough to provide a sufficient signal-to-noise ratio.

As already mentioned, Figure 2 depicts the response of the native color pixels, and it is obvious that any light with a wavelength longer than 670 nm cannot be identified by the camera algorithm as dark red light because the blue and green channels give a signal as well. However, in order to provide an acceptable detection of ‘red’ light, the red channel needs a steep transition from high transmittance at 600 nm and blocking at 670 nm to obtain enough ‘red light’.

In order to obtain an enhanced NIR-cutoff filter, the two systems are combined: as a substrate, a filter glass is used (e.g., blue glass BG60 [5]), which is coated from one side with a broadband anti-reflection (AR) coating for

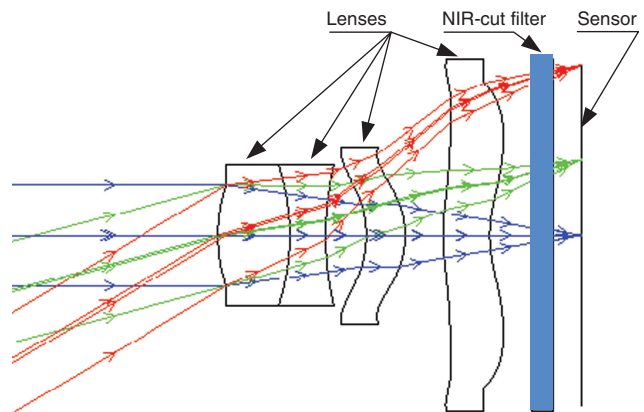


**Figure 4** Typical optical design of a digital camera in smart phones [3]. The NIR cut filter is the plano-parallel plate (blue) next to the image sensor on the right. Design data: F number=2.8, an effective focal length of 4.028 mm, a total length of 5.083 mm, and a field of view of ±31.2°.

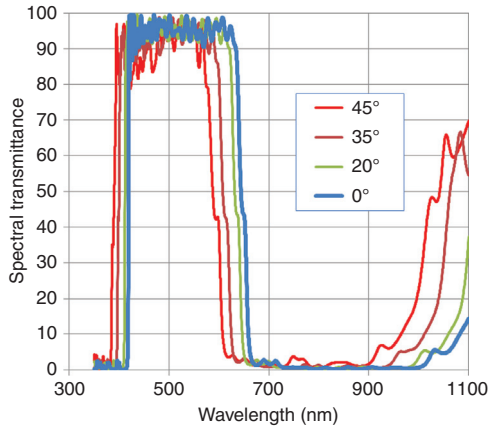


**Figure 5** Example of a design of an interference filter based on a substrate made of clear glass (N-BK7). The spectral transmittance is given for different angles of incidence.

the visible range. The second surface of the filter glass is coated with a special interference coating that has three functions:

1. it has to provide AR properties in the range of 380 nm –650 nm;
2. it has to serve as a UV-cutoff filter for all wavelengths shorter than 380 nm; and
3. it has to provide additional NIR-cutoff properties to the filter glass.

Figure 7 compares the spectral properties of the uncoated filter glass to the optimized combination made from filter glass and interference coatings: the optical filter glass is coated on one side with a broad band AR coating and on the other side with an interference filter. The effect on the performance concerning transmittance can easily be seen.

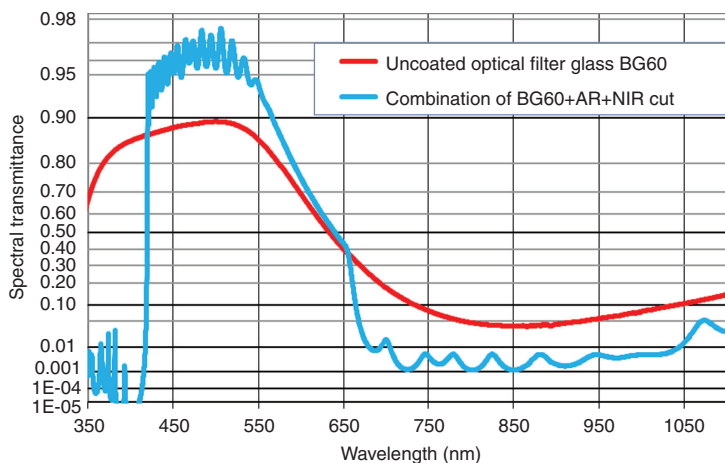


**Figure 7** Spectral transmittance (in diabolic scale) of uncoated BG60 filter glass at a thickness of 0.3 mm and of coated BG60 filter glass with anti-reflection coating and additional NIR cut coating. The transmittance of the coated filter is calculated using [4]. The data of the uncoated filter glass was taken from [5].



**Figure 6** Picture of two candles with ghost images. The ghosts are reflections of the hot regions of the flame that are upside down. The picture was taken with a 6-megapixel DSC camera.

The typical thickness of the filter glass is 0.3 mm, which has a maximum transmittance of almost 90% at 500 nm and <10% transmittance for most of the NIR. This enables a miniaturized design with high absorption but still much transmittance in the visible region between 400 nm and 650 nm.

The spectral absorption and the internal transmission of filter glasses are a function of the thickness, obeying:

$$\tau_i(\lambda) = e^{-\alpha(\lambda)d}, \tag{1}$$

where  $\tau_i$  is the internal transmittance (without two surface Fresnel losses);  $\alpha$  is the spectral absorption coefficient, and  $d$  is the thickness of the filter glass. This means there is a tradeoff for high absorption: in case the designer increases the thickness of the filter, higher absorption is obtained (to reduce stray light). But such a thicker filter will also reduce the transmittance in the visible, which

will lower the sensitivity of the camera in a low-light environment.

Thus, the design of the filter thickness depends on the native pixel response and the desired low light sensitivity of the camera (lens system and sensor).

### 3.1 Tolerance analysis for small variations in the transmittance of the filter glass

Typically, an interference coating is optimized for a typical transmittance curve of the absorbing filter glass (blue glass). The transmission spectrum of such an absorbing filter glass (blue glass) has small variations due to production variations (although glass manufacturer reduce this variations as small as possible). Transmittance variations due to manufacturing of the interference filter coating are typically smaller than the transmittance variations of the absorbing filter glass due to optical monitoring during the interference filter production. The effect of the transmittance curve variation on the performance is now examined. The slope of the transmittance curve at the NIR-cutoff is the most sensitive parameter, and small variations of the cutoff wavelength have a huge effect on the color calculation. (The cutoff wavelength  $\lambda_{0.5}$  is the wavelength at which the transmittance is equal to 0.5). Figure 8 visualizes the effect of small variations: differences in the coated filters are significant in the range between 540 nm and 650 nm, only. Those variations will change the response of the red and green color channels, which will cause deviations in the color calculation algorithm. The color that the camera is sensing is basically an integration of the filtered light where every pixel is filtered by the color filter of the native pixel and the NIR cut filter.

An integration of the transmittance of NIR-cut filter over the CIE color-matching functions using an equi-energy spectrum gives a good approximation of the variations of the color locus. Using the CIE (1976) UCS color coordinates [1], one can derive a radius of tolerance for the color locus depending on the tolerance of the cutoff wavelength of the filter glass. Table 1 shows the results of the color analysis.

The radius of tolerance of the color locus is a measure for the color variations. According to MacAdam's measurements (data taken from [6]), a human cannot detect any color difference for an area in the UCS color diagram of an approximate radius of 0.001. Thus, the results shown in Table 1 are well above the value reported by MacAdam. However, a radius of tolerance for the color locus of 0.003 is usually acceptable because it is a reasonable compromise between manufacturing efforts and subjective color recognition by the human eye.

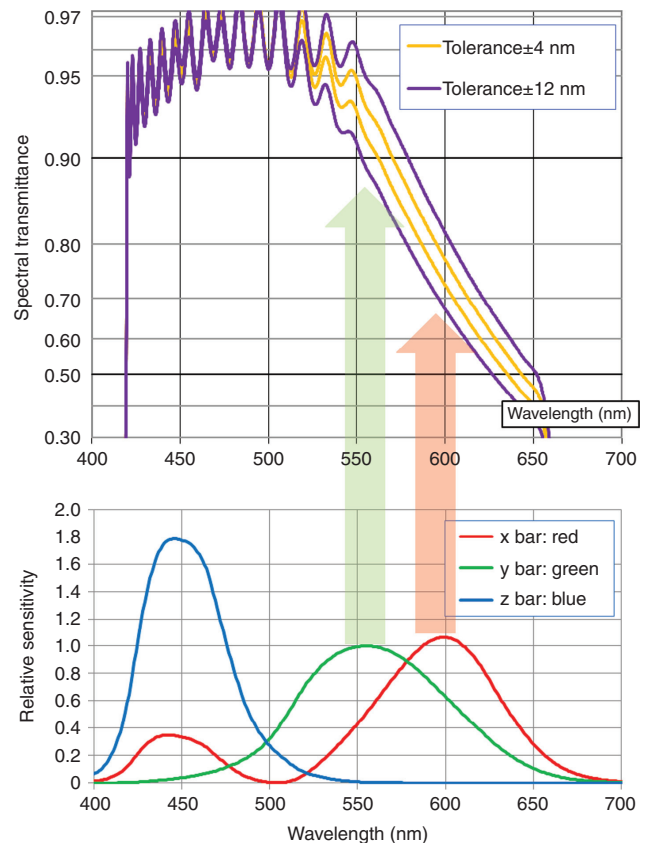


**Figure 8** Effect of variations in cutoff wavelength  $\lambda_{0.5}$  on the transmittance of the coated filter (top – in diabolic scale), which influences significantly the color calculation of the green and red color channels (bottom – in linear scale). The red and green arrows indicate the biggest effect of the transmittance curve on the color calculation, when the color is derived by integrating the transmittance over the red and green color channels, respectively. Variations of the transmittance have no significant effect on the calculation of the blue channel.

## 4 Special optical properties of the filter glass

Filter glasses for imaging applications have to satisfy not only tight tolerances of cutoff wavelength. Additionally, such glasses need to have repeatable refractive index, very good inner quality and homogeneity, and good climatic resistance. Because those filters are placed right in

**Table 1** Calculation results for the tolerance radius of the color locus using CIE UCS coordinate system.

Tolerance of the cutoff wavelength $\lambda_{0.5}$	±4 nm	±8 nm	±12 nm
Radius of color locus in UCS coordinates	0.002	0.004	0.006

The results are calculated as a function of different variations of the optical filter glass.

front of the sensor (see Figure 4), any obstacle will mask out some pixels of the sensor. Therefore, the filter must have very low surface defects, inclusions, or bubbles. Low surface defects automatically need sophisticated lapping and polishing processes and cleaning of the filter glass.

#### 4.1 Importance of refractive index

The refractive index over wavelength of the plano-parallel optical filter plate has to be known either for the optical design, and as well, for the NIR interference filter design. Therefore, the refractive index has to be measured not only in the visible region but also in the range of the NIR, which enables an optimized design of the interference filter from 650 nm on. However, it is difficult to measure the refractive index of absorbing filter glass like BG60 as it blocks light between about 700 nm and 1000 nm. This means no signal can be detected, and so, no refractive index can be measured. Usually, refractometric measurement or reflectometric measurements were used, but not a combination of both. Here, we used both results from refractometric and reflectometric measurement techniques, which were combined to measure the refractive index (see Figure 9). Subsequently, the data was fitted to a Sellmeier formula in order to get refractive indices for the whole range from 350 nm to 1550 nm – see Figure 9, which contains both measurement data and Sellmeier representation of the refractive index.

The three-term Sellmeier fit of the measured refractive index is given by:

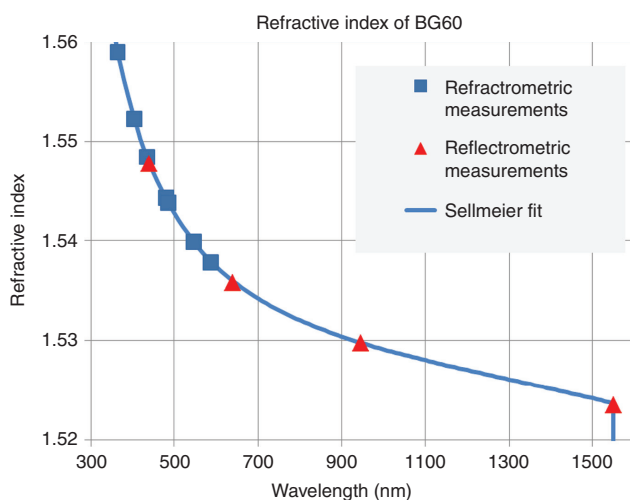


**Figure 9** Refractive index vs. wavelength of BG60 absorbing filter glass. The deviation of the Sellmeier fit to the measured data is of order 0 (0.00052), and the uncertainty of the measurement is  $\pm 0.0005$ .

$$n^2(\lambda)-1 = \frac{B_1\lambda^2}{\lambda^2-C_1} + \frac{B_2\lambda^2}{\lambda^2-C_2} + \frac{B_3\lambda^2}{\lambda^2-C_3}, \quad (2)$$

where  $\lambda$  is the wavelength,  $n$  is the refractive index, and  $B_{1...3}$  and  $C_{1...3}$  are the coefficients given in Table 2.

It should be noted that a Sellmeier series assumes a lossless, i.e., absorption-free material – which is not the case for BG60 absorbing filter glass. But the imaginary part of the refractive index – describing the absorption for BG60 – is more than a factor of 1000 smaller at 800 nm (high-absorption region) than the real part. Therefore, the imaginary part of the refractive index can be neglected. This means the Sellmeier series (assuming lossless material) can also be applied to the absorbing filter glass BG60! The Sellmeier fit together with the measured data of the refractive index can be seen in Figure 9.

With the help of the Sellmeier representation of the refractive index, the Abbe number  $v_d$  and the partial dispersion  $P_{g,F}$  of BG60 can be found to be:

$$v_d = \frac{n_d - 1}{n_F - n_C} = 64.6 \quad (3)$$

$$P_{g,F} = \frac{n_g - n_F}{n_F - n_C} = 0.556, \quad (4)$$

with  $n_d$  the refractive index at the Fraunhofer  $d$ -line (587.6 nm). Accordingly,  $F$ -line is at 486.1 nm,  $C$ -line is at 656.3 nm, and  $g$ -line is at 435.8 nm.

#### 4.2 Effect of striae in a NIR filter

The internal quality of glasses are studied here in terms of striae. Striae are defined as short length – typically between 0.1 mm and 1.0 mm – fluctuations of the refractive index (compare with [7]) due to locally small changes in the chemical composition. If a plane wave hits a plano-parallel glass plate (such as a NIR filter shown in

**Table 2** Sellmeier coefficients of BG60.

$B_1$	1.23258101	$1/\mu\text{m}^2$
$B_2$	0.09947665	$1/\mu\text{m}^2$
$B_3$	0.06247848	$1/\mu\text{m}^2$
$C_1$	0.00657797	$\mu\text{m}^2$
$C_2$	0.03470719	$\mu\text{m}^2$
$C_3$	12.2405947	$\mu\text{m}^2$

The fit is valid in the range 340 nm–1550 nm.

Note:  $\lambda$  must be used in unit  $\mu\text{m}$  for the fit.

Figure 4), then, a local change in the refractive index leads to a wavefront deformation. Therefore, striae will cause wavefront deformation and will affect the imaging quality of the camera system. A wavefront deformation  $\Delta\varphi$  can be related to an optical path difference  $\Delta L$  according [8, 9]:

$$\Delta L = \frac{\Delta\varphi \cdot \lambda_0}{2\pi}, \quad (5)$$

where  $\lambda_0$  is the wavelength of light in vacuum. Typically, striae are clustered (see e.g., [10]), and according to a SCHOTT internal definition, an optical path difference of  $\Delta L=0$  nm...10 nm corresponds to an 'A' striae ( $\Delta L=10$  nm...15 nm = 'B' striae,  $\Delta L=15$  nm...30 nm = 'C' striae,  $\Delta L=30$  nm...60 nm = 'D' striae).

In order to study the effect of wavefront deformation due to striae, the optical design shown in Figure 4 is used. Details of the design can be found in [3] and [11]. A typical design software like [12] cannot directly model striae, but height fluctuations (see also [13]). An optical path difference  $\Delta L$  can be modeled as height fluctuations  $\Delta h$  (assuming a perfect glass without striae) by:

$$\Delta h = \frac{\Delta L}{n-1}, \quad (6)$$

where  $n$  is the refractive index of the absorbing filter glass (for BG60:  $n_d=1.5399$ ). According to Eq. (6), a D striae with maximum optical path difference of 60 nm, corresponds to a maximum surface fluctuation of 112 nm.

The effect of striae inside an absorption filter glass is now modeled as surface fluctuation as illustrated in Figure 10. The design software ZEMAX [12] provides a surface type called 'periodic surface,' which can be used for this. Here, the peak to valley fluctuation corresponds to the height fluctuation  $\Delta h$ . A worst case simulation thus

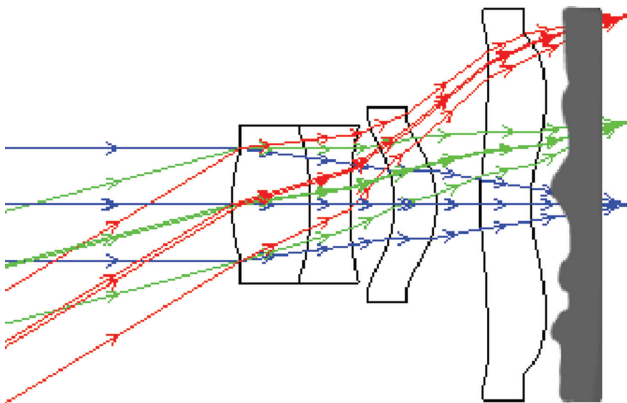


**Figure 10** Modeling striae in a NIR absorption filter as height fluctuation (illustration).

uses a peak to valley fluctuation of 112 nm for a D striae (as maximum).

The effect of the design with and without striae is simulated where the refractive index data for BG60 were given according Table 2. The parameters of the four lenses are those given in [3]. As a parameter, the spot size (radius) of the central spot (field at  $0^\circ$  incidence – blue rays in Figure 10) and the most outward spot size (at  $31.2^\circ$  incidence – red rays in Figure 10) were investigated, and the results are summarized in Table 3.

As seen from Table 3, the effect of striae is small, but changes the spot size (radius) by 10% for a D striae for the center spot. The most outward spot (at  $31.2^\circ$  incidence) is unchanged. But this does not mean that the filter glass can have massive striae. A surface fluctuation of 300 nm will cause a spot size (radius) of  $1.2 \mu\text{m}$  and, thus, 20% change for the central spot. Therefore, striae inside an absorption NIR cut filter should be equal or less than D striae.

## 5 Absorption filter lens for reduced length and effect on color

Instead of using a coated absorption filter glass as a plano-parallel plate in front of the sensor, the optical position of  $n_d=1.5399$  and  $v_d=64.6$  suggests to use it as an optical lens. Such an optical position is suited for chromatic correction by using it as a crown glass in an achromate [11]. Thus, the filter function as well as achromatic feature can be combined by making the first lens out of an absorption filter glass. This, in turn, means the plano-parallel filter plate in front of the sensor can be omitted reducing the overall size and making the assembly of the lens system significantly easier. Figure 11 illustrates this.

Of course, the lens-filter combination is again made from absorption filter glass and an interference coating. In this case, the interference coating is placed on the first surface of the lens barrel. Thus, all reflections of the coating will be redirected away from the lens system. This reduces the danger of ghost images even more.

In order to get the same filter function, the absorption filter glass must be adopted. The absorption for such

**Table 3** Design results for striae inside absorbing filter glass (in terms of spot radius).

Parameter	Ideal case	D striae ( $\Delta h=112$ nm)
Spot size (radius), field at $0^\circ$	$1.0 \mu\text{m}$	$1.1 \mu\text{m}$
Spot size (radius), field at $31.2^\circ$	$3.6 \mu\text{m}$	$3.6 \mu\text{m}$

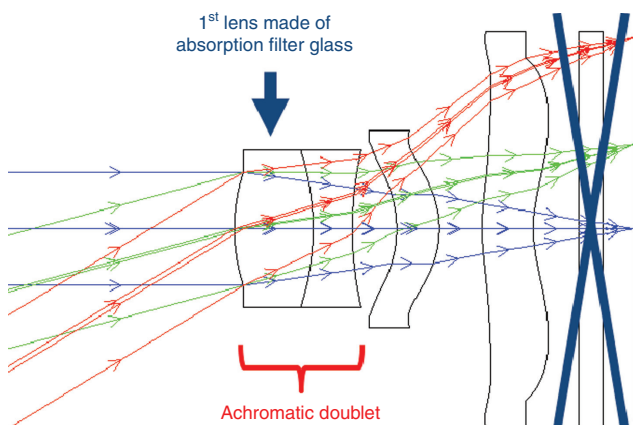


**Figure 11** An optical design using an absorption filter glass lens (first lens – e.g., BG63) does not need any longer a flat plate filter and takes over the role as a crown glass inside an achromatic lens doublet.

a blue glass is typically done by adding copper oxide, and therefore, the copper oxide concentration must be reduced in order to obtain the same absorption as within a thin flat plate filter (see [11]). Surprisingly, such a blue glass absorption filter first lens leads to the same results in the required filter function (by adopting the copper oxide concentration) as in a standard design.

BG63 is another blue filter glass (absorption filter) that has approximately the required filter function for the 1-mm-thick (center thickness) first lens. This means a 1-mm-thick BG63 first lens has nearly the same filter function as the 0.3-mm-thick BG60 plano-parallel filter plate.

It turns out that the internal quality of such an absorption filter lens needs to be better than for a flat plate filter. A detailed analysis [11] shows that already a type B striae with up to 30 nm optical path difference increases the central spot size (spot radius at  $0^\circ$  incidence) to  $1.5 \mu\text{m}$ . Therefore, the absorption filter glass must have optical quality, and a Sellmeier representation of the refractive index is also needed for such a purpose.

The first lens of the design in Figure 11 has a center thickness of 1.0 mm, and the center rays (at  $0^\circ$  incidence) traverse the lens at 1.0 mm thickness (central blue ray in Figure 11) and at 0.835 mm thickness (outer blue ray in Figure 11). By traveling through the absorption filter lens at different optical path lengths, the rays of the center are subject to higher absorption than the rays that travel through glass at the border of the lens (outer blue ray in Figure 11).

However, this difference in absorption has only a small effect on the color recognition of the system. Figure 12 shows the difference for a coated lens made from BG63. BG63 has less color concentration than BG60,

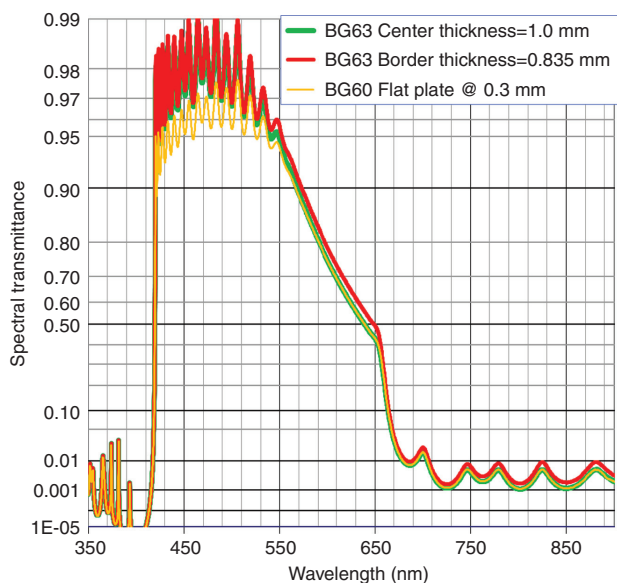


**Figure 12** Spectral transmittance of single rays traveling through a lens made from BG63. The transmittance is given for the center ray at an angle of incidence =  $0^\circ$  and for the rays at the border of the lens, which have a minimum length of the optical path = 0.835 mm. For comparison, the transmittance of a flat plate filter made from BG60 is depicted (see Figure 7). All components have the same optical coatings.

and therefore, the lens can be produced at a reasonable center thickness of 1 mm, without absorbing too much light. For comparison, Figure 12 depicts the transmittance of the coated flat plate filter of the standard design (see Figure 7).

The shown differences in transmittance are worst case differences of particular rays. However, the light that hits a single pixel of the sensor is the sum of many rays that are focused by the lens onto that particular pixel. Thus, the transmittance of the lens is an integral value, which lies between those two graphs for the center ray and the border rays, respectively. This means that the variations shown in Figure 12 will not add to the variations in Figure 8 and, therefore, will not have any effect on the color recognition of the camera system.

## 6 Summary and conclusion

The function of NIR-cutoff filters for color recognition of digital cameras has been explained, and the advantages of using a combination of an absorption filter glass and an optimized interference coating has been described.

In such a combined filter, the optical properties transmittance and striae are of special importance; therefore,

their influence on image quality and color recognition has been analyzed.

NIR-cutoff filter may be designed as a flat plate component or as a lens that reduces the number of components in a lens system. It is shown that the design is feasible and that the lens-filter combination has the same performance as a flat plate filter concerning true color transmittance and reducing ghost images.

**Acknowledgment:** For the support of this work, we would like to acknowledge our colleagues Thea Marcoux, Bianca Schreder, Ralf Reiter, Volker Dietrich, Frank-Thomas Lentès, and Ulf Brauneck. We also thank the reviewer for his valuable comments.

Received July 10, 2013; accepted September 2, 2013; previously published online October 5, 2013

## References

- [1] Commission Internationale de l'Eclairage: CIE15; 2004, 3rd ed. ISBN 3901906339.
- [2] Eastman Kodak Comp.; Application Note: Color correction for image sensors; Revision 3.0 MTD/PS-0534; August 13, 2008.
- [3] Y. Choi, S. Jeong, S. Kim, 'Lens system for ultra-small camera module and image forming lens with infrared filtering function used therefore', US patent, Example described in table 7 and 8, US 2007/0024958 A1, 2007.
- [4] Interference filter design software: OptiLayer Thin Film Software, OptiLayer Ltd. Alexander V. Tikhonravov, Michael K. Trubetskoy; 2013, see <http://www.optilayer.com/general.htm>.
- [5] SCHOTT optical filter glass calculation tool, SCHOTT AG, Mainz, Germany, 2013; see [http://www.schott.com/advanced\\_optics/english/download/schott-filter-glass\\_2013.xlsx](http://www.schott.com/advanced_optics/english/download/schott-filter-glass_2013.xlsx).
- [6] G. Wyszecki, W.S. Stiles, Color Science: Concepts and Methods, Quantitative Data and Formula, 2nd ed. (Wiley-Interscience, July 28, 2000). ISBN 0-471-39918-3.
- [7] See Standard ISO 10110 – part 4.
- [8] E. Hecht, Optik (2. Auflage). (Oldenbourg Verlag, München, 1999).
- [9] M. Born, E. Wolf, Principles of Optics, 7th ed. (Cambridge University Press, Cambridge, 1999).
- [10] See Standard MIL-G-174B.
- [11] S. Reichel, F.-T. Lentès, Blue glass lens elements used as IR cut filter in a camera design and the impact of inner quality onto lens performance, paper 8550-24, SPIE Proceedings Vol. 8550, SPIE Optical Systems Design, Barcelona, Spain, Nov. 2012.
- [12] Optical design software Zemax, Radiant Zemax, see <http://www.radiantzemax.com>, 2013.
- [13] D. Hill, How To Tolerance for Material Inhomogeneity. ZEMAX knowledge base, December 16, 2005, see <http://kb-en.radiantzemax.com/Knowledgebase/>.



Dr. Ralf Biertümpfel studied Mechanical and Aerospace Engineering at the Technical University of Darmstadt (Germany) and Cornell University (USA). After his diploma and his Master of Engineering in 1996, he worked on a research project in the field of heat transfer and thermodynamics and finally earned his doctorate at the Technical University of Darmstadt in 2001. Since 2001, he works at SCHOTT AG in the fields of hot forming of glass and precision optics. At present, he is the application manager for optical filters.



Steffen Reichel studied Electrical Engineering at the University of Kaiserslautern and spend 7 months at the Michigan State University, Michigan, USA. After his diploma degree in 1996, he worked as a researcher at the University of Kaiserslautern working on his doctorate (Dr.-Ing.) in the field of optical communications (fiber optics, erbium-doped fiber amplifiers). In 1999, he joined Lucent Technologies working on fiber optical communications, erbium-doped, and Raman amplifiers. Since 2001, he works for SCHOTT on several fields of optics from imaging optics, fiber optics, waveguide optics, laser optics, illumination optics, and optical filters. He is a Senior Member of the IEEE and Member of the SPIE, and since 2013, he is a professor (honorary) for 'Optics & Photonics' at the University of Applied Science, Darmstadt, Germany. In addition, he is co-author in three books, has about 60 publications, and has 20 granted or applied patents.